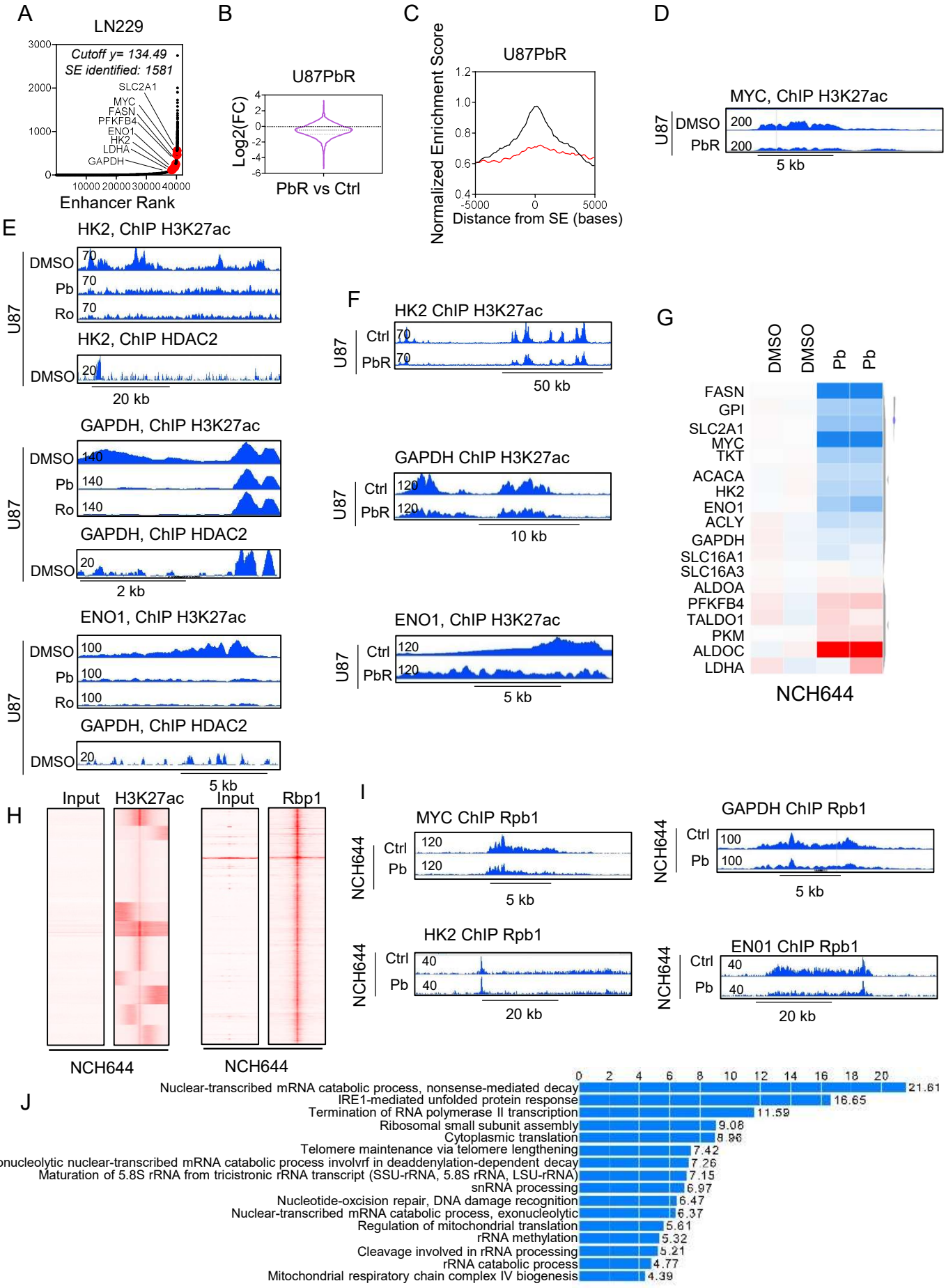
A
LN229
Cutoff y= 134.49
SE identified: 1581
SLC2A1
MYC
FASN
PFKFB4
ENO1
HK2
LDHA
GAPDH
Enhancer Rank
B
U87PbR
Log2(FC)
PbR vs Ctrl
C
U87PbR
Normalized Enrichment Score
Distance from SE (bases)
D
MYC, ChIP H3K27ac
U87
DMSO
PbR
5 kb
E
HK2, ChIP H3K27ac
HK2, ChIP HDAC2
GAPDH, ChIP H3K27ac
GAPDH, ChIP HDAC2
ENO1, ChIP H3K27ac
GAPDH, ChIP HDAC2
U87
DMSO
Pb
Ro
20 kb
2 kb
5 kb
F
HK2 ChIP H3K27ac
GAPDH ChIP H3K27ac
ENO1, ChIP H3K27ac
U87
Ctrl
PbR
50 kb
10 kb
5 kb
G
DMSO
DMSO
Pb
Pb
FASN
GPI
SLC2A1
MYC
TKT
ACACA
HK2
ENO1
ACLY
GAPDH
SLC16A1
SLC16A3
ALDOA
PFKFB4
TALDO1
PKM
ALDOC
LDHA
NCH644
H
Input
H3K27ac
Input
Rbp1
NCH644
NCH644
I
MYC ChIP Rpb1
GAPDH ChIP Rpb1
HK2 ChIP Rpb1
EN01 ChIP Rpb1
NCH644
Ctrl
Pb
5 kb
20 kb
J
Nuclear-transcribed mRNA catabolic process, nonsense-mediated decay 21.61
IRE1-mediated unfolded protein response 16.65
Termination of RNA polymerase II transcription 11.59
Ribosomal small subunit assembly 9.08
Cytoplasmic translation 8.96
Telomere maintenance via telomere lengthening 7.42
Exonucleolytic nuclear-transcribed mRNA catabolic process involvrf in deaddenylation-dependent decay 7.26
Maturation of 5.8S rRNA from tricistronic rRNA transcript (SSU-rRNA, 5.8S rRNA, LSU-rRNA) 7.15
snRNA processing 6.97
Nucleotide-oxcision repair, DNA damage recognition 6.47
Nuclear-transcribed mRNA catabolic process, exonucleolytic 6.37
Regulation of mitochondrial translation 5.61
rRNA methylation 5.32
Cleavage involved in rRNA processing 5.21
rRNA catabolic process 4.77
Mitochondrial respiratory chain complex IV biogenesis 4.39

Figure S1: Identification of super-enhancers in the desert of Warburg-related genes, which are disrupted by HDAC inhibitors. (A) Chromatin immunoprecipitation with H3K27Ac coupled with next generation sequencing was performed in LN229 cells. Shown are the super-enhancers of genes involved in glycolysis, the pentose phosphate pathway and fatty acid synthesis. (**B** and **C**) A representation of global disruption of the super-enhancer landscape of parental and chronically panobinostat (Pb) exposed U87 cells (SE: super enhancer). (**D**) ChIP-sequencing (H3K27ac) was performed in parental and chronically exposed panobinostat U87 cells. Shown are the respective tracks around the indicated genes (pile up values are indicated). (**E**) ChIP sequencing (H3K27ac) was performed in panobinostat /romidepsin (Ro) treated U87 cells (24 h treatment). Shown are the respective tracks around the HK2, GAPDH and ENO1. (**F**) ChIP-sequencing (H3K27ac) of parental and chronically panobinostat exposed U87 GBM cells. Shown are the respective tracks around the HK2 and GAPDH loci. (**G**) NCH644 cells were treated with 0.5 μM panobinostat for 24h followed by RNA extraction. RNA was processed for microarray analysis. A heat map of genes related to the Warburg effect consists of genes encoding for enzymes or transporters involved in glycolysis, the pentose phosphate pathway and fatty acid synthesis. (**H**) Heat maps from inputs and CHIPs (H3K27ac and Rpb1) performed on chromatin from NCH644 GBM cells. The peak centers are displayed +/- 5kb. (**I**) ChIP sequencing profile (antibody Rpb1) of panobinostat treated NCH644 GBM cells. Shown are the respective tracks around the MYC, HK2, GAPDH and ENO1 loci. (**J**) Shown is the gene ontology analysis of CHIP-seq (Rpb1) in NCH644 treated with 0.5 μM panobinostat for 24h.

Figure S2

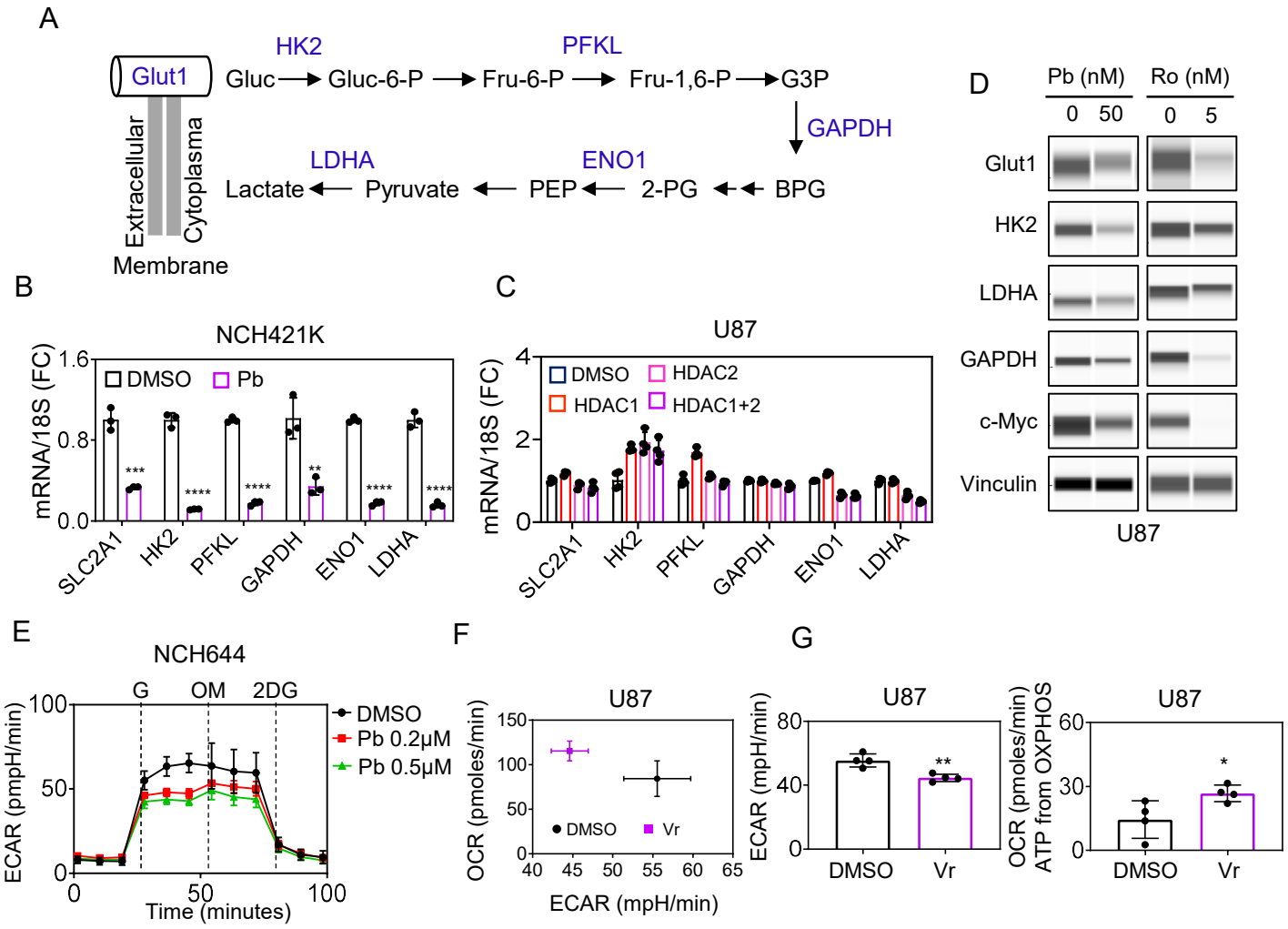
A
Glut1
HK2
PFKL
Gluc
Gluc-6-P
Fru-6-P
Fru-1,6-P
G3P
GAPDH
LDHA
ENO1
Lactate
Pyruvate
PEP
2-PG
BPG
Extracellular
Cytoplasma
Membrane
B
NCH421K
mRNA/18S (FC)
DMSO
Pb
SLC2A1
HK2
PFKL
GAPDH
ENO1
LDHA
C
U87
DMSO
HDAC2
HDAC1
HDAC1+2
D
Pb (nM)
Ro (nM)
0
50
0
5
Glut1
HK2
LDHA
GAPDH
c-Myc
Vinculin
U87
E
NCH644
G
OM
2DG
ECAR (pmpH/min)
DMSO
Pb 0.2μM
Pb 0.5μM
Time (minutes)
F
U87
OCR (pmoles/min)
DMSO
Vr
ECAR (mpH/min)
G
U87
ECAR (mpH/min)
DMSO
Vr
U87
OCR (pmoles/min)
ATP from OXPHOS
DMSO
Vr

Figure S2: HDAC inhibitors suppress glycolysis and associated biosynthetic pathways. **(A**) Summary chart of the enzymes and transporters down regulated in the glycolytic pathway in NCH644 stem-like GBM cells. Blue indicates a suppression of the respective protein in panobinostat treated samples. (**B**) Real-time PCR analysis of genes related to glycolysis from stem-like NCH421K GBM cells treated with 0.1 μM panobinostat for 24h (n=3). (**C**) Real-time PCR analysis of genes related to glycolysis from U87 GBM cells transfected with siRNA against HDAC1, HDAC2, or the combination of both (n=4). (**D**) Protein capillary electrophoresis analysis of lysates from U87 cells that were treated with 50 nM panobinostat or 5 nM romidepsin for 24h. (**E**) NCH644 cells were treated with the indicated concentrations of panobinostat and glycolysis stress extracellular flux analysis was performed. (**F** and **G**) U87 cells were treated with Vorinostat (Vr) and OCR and ECAR measurements were performed. Shown are means and SD. Statistical significance was determined by two-tailed Student's t-test. *P < 0.05; **P < 0.01; ***/****P < 0.001.

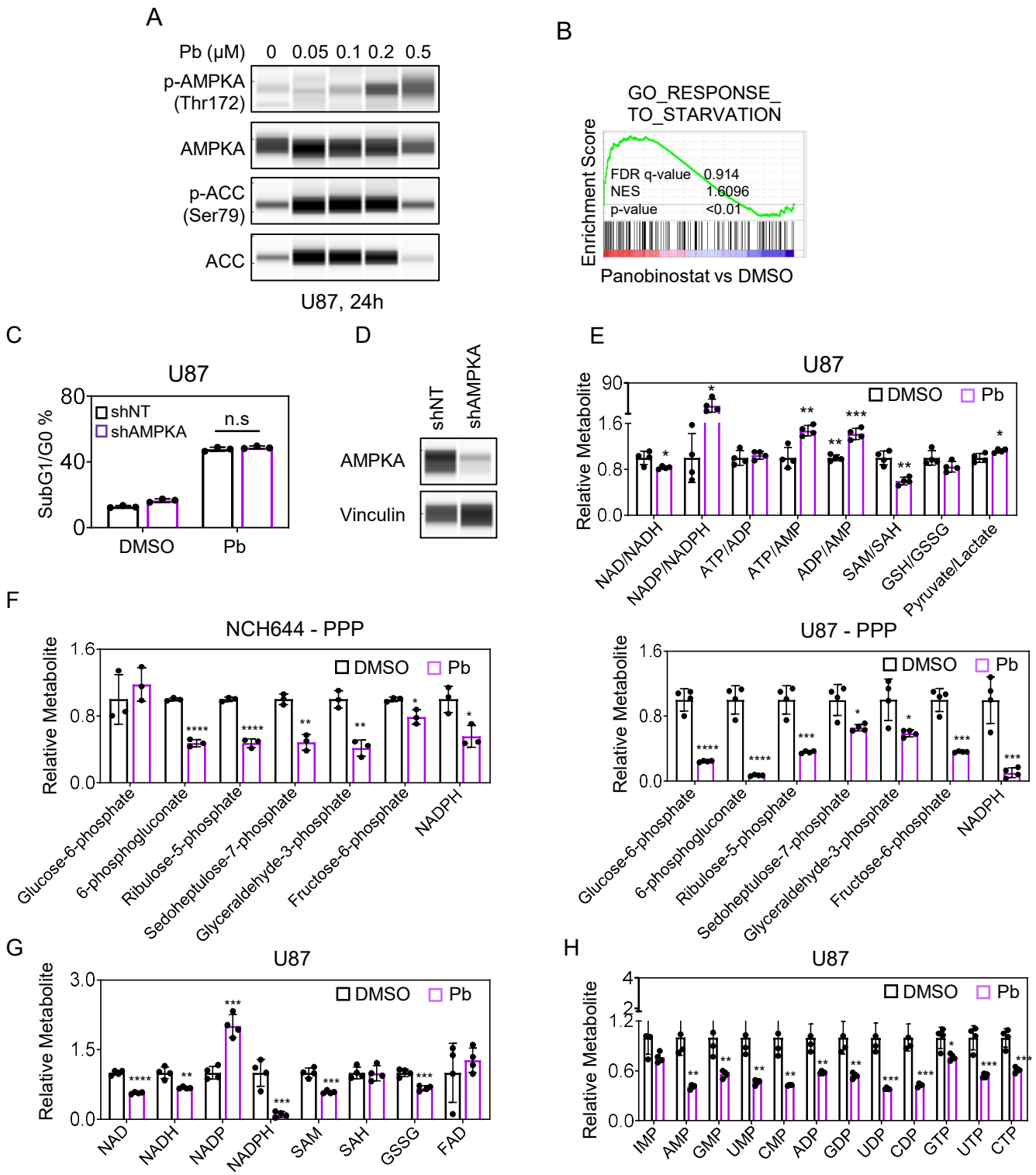
A
Pb (μM) 0 0.05 0.1 0.2 0.5
p-AMPKA (Thr172)
AMPKA
p-ACC (Ser79)
ACC
U87, 24h
B
GO_RESPONSE_ TO_STARVATION
Enrichment Score
FDR q-value 0.914
NES 1.6096
p-value <0.01
Panobinostat vs DMSO
C
U87
SubG1/G0 %
shNT
shAMPKA
n.s
DMSO
Pb
D
shNT
shAMPKA
AMPKA
Vinculin
E
U87
Relative Metabolite
DMSO
Pb
NAD/NADH
NADP/NADPH
ATP/ADP
ATP/AMP
ADP/AMP
SAM/SAH
GSH/GSSG
Pyruvate/Lactate
F
NCH644 - PPP
Relative Metabolite
DMSO
Pb
Glucose-6-phosphate
6-phosphogluconate
Ribulose-5-phosphate
Sedoheptulose-7-phosphate
Glyceraldehyde-3-phosphate
Fructose-6-phosphate
NADPH
U87 - PPP
Relative Metabolite
DMSO
Pb
Glucose-6-phosphate
6-phosphogluconate
Ribulose-5-phosphate
Sedoheptulose-7-phosphate
Glyceraldehyde-3-phosphate
Fructose-6-phosphate
NADPH
G
U87
Relative Metabolite
DMSO
Pb
NAD
NADH
NADP
NADPH
SAM
SAH
GSSG
FAD
H
U87
Relative Metabolite
DMSO
Pb
IMP
AMP
GMP
UMP
CMP
ADP
GDP
UDP
CDP
GTP
UTP
CTP

Figure S3: Panobinostat suppresses the pentose phosphate pathway and the levels of purine and pyrimidine nucleotides. (A) Capillary electrophoresis of proteins from U87 cells treated with the indicated concentrations of panobinostat for 24h. (**B**) GO_RESPONSE_TO_STARVATION GSEA results of NCH644 cells treated with panobinostat. NES: normalized enrichment score. (**C**) U87 cells were transduced with AMPKA shRNA lentivirus. Cells were exposed to panobinostat and analyzed for apoptosis (n=3). (**D**) Protein capillary electrophoresis analysis of lysates from U87 cells that were transduced with AMPKA shRNA lentivirus. **(E)** U87 cells were treated with 0.5 μM panobinostat. Cells were subjected to LC/MS analysis for the indicated metabolites. (**F**) NCH644 and U87 GBM cells were treated with 0.5 μM panobinostat (U87 cells) or 0.5 μM panobinostat (NCH644 cells) for 24h. Cells were subjected to LC/MS analysis for the indicated metabolites related to the pentose phosphate pathway (PPP), nucleotides and redox related metabolites (n=3). (**G** and **H**) U87 cells were treated with 0.5 μM panobinostat for 24h and subjected to LC/MS analysis for the indicated metabolites (n=4). Shown are means and SD. Statistical significance was determined by two-tailed Student's t-test. *P < 0.05; **P < 0.01; ***/****P < 0.001.

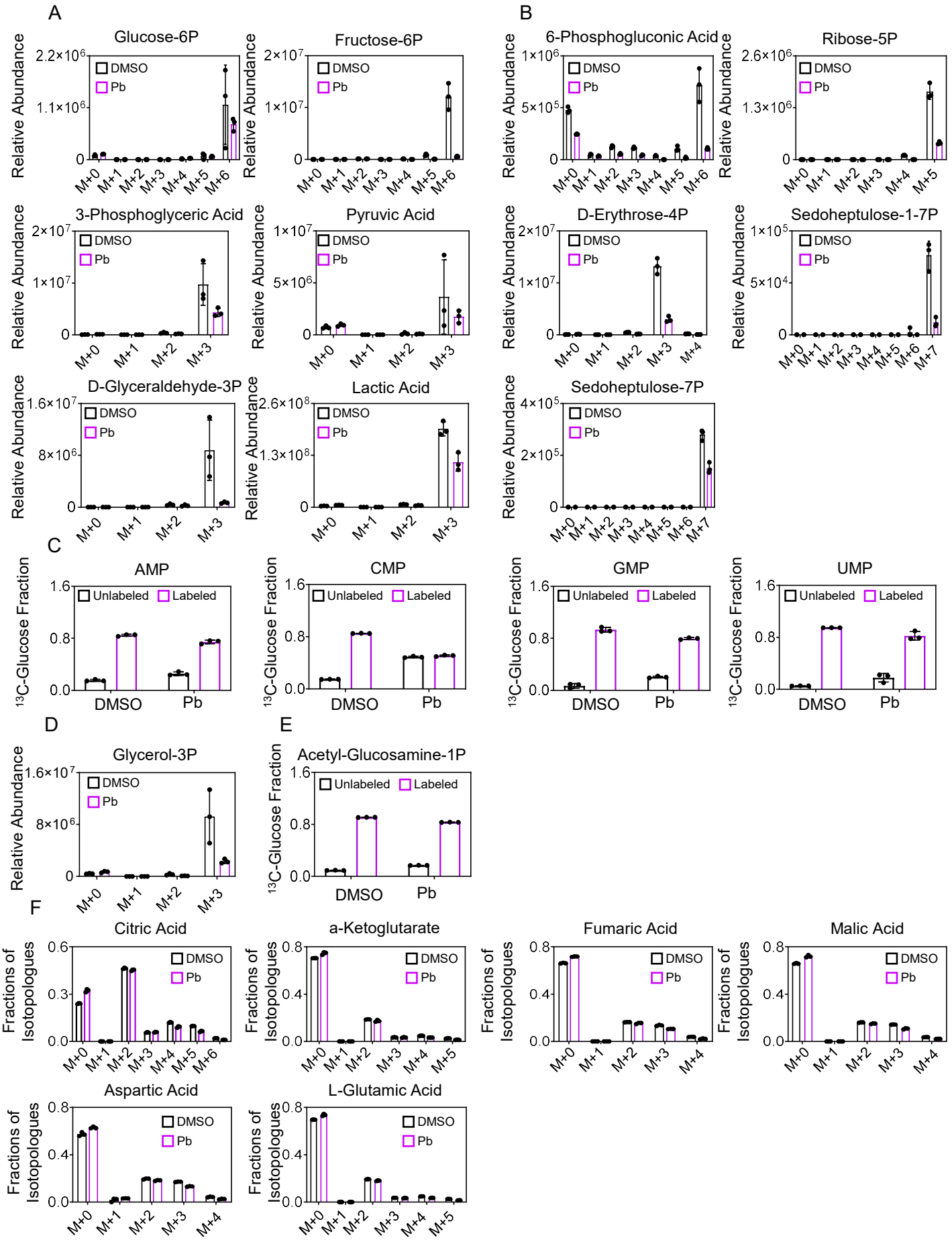
A
Glucose-6P
Fructose-6P
3-Phosphoglyceric Acid
Pyruvic Acid
D-Glyceraldehyde-3P
Lactic Acid
B
6-Phosphogluconic Acid
Ribose-5P
D-Erythrose-4P
Sedoheptulose-1-7P
Sedoheptulose-7P
C
AMP
CMP
GMP
UMP
D
Glycerol-3P
E
Acetyl-Glucosamine-1P
F
Citric Acid
a-Ketoglutarate
Fumaric Acid
Malic Acid
Aspartic Acid
L-Glutamic Acid
Relative Abundance
Fractions of Isotopologues
^{13}C-Glucose Fraction
DMSO
Pb
Unlabeled
Labeled
M+0
M+1
M+2
M+3
M+4
M+5
M+6
M+7

Figure S4: Panobinostat reduces carbon labeling (U-^{13}C-glucose) of metabolites related to the pentose phosphate pathway, lipid synthesis, hexosamine biosynthesis, nucleotide synthesis, and TCA cycle. (A-F) U87 GBM cells were treated with 0.5 μM panobinostat in the presence of 25 mM U-^{13}C-glucose, 4 mM glutamine and 1.5% dialyzed FBS. After 24h, cells were harvested and analyzed by LC/MS. Shown are the relative abundances of ^{13}C labeled each isotopologues from U-^{13}C-glucose for the indicated metabolites related to glycolysis (A), pentose phosphate pathway (B), nucleotides (C), lipid synthesis (D), hexosamine biosynthesis (E), TCA-cycle (F) (n=3). Shown are means and SD.

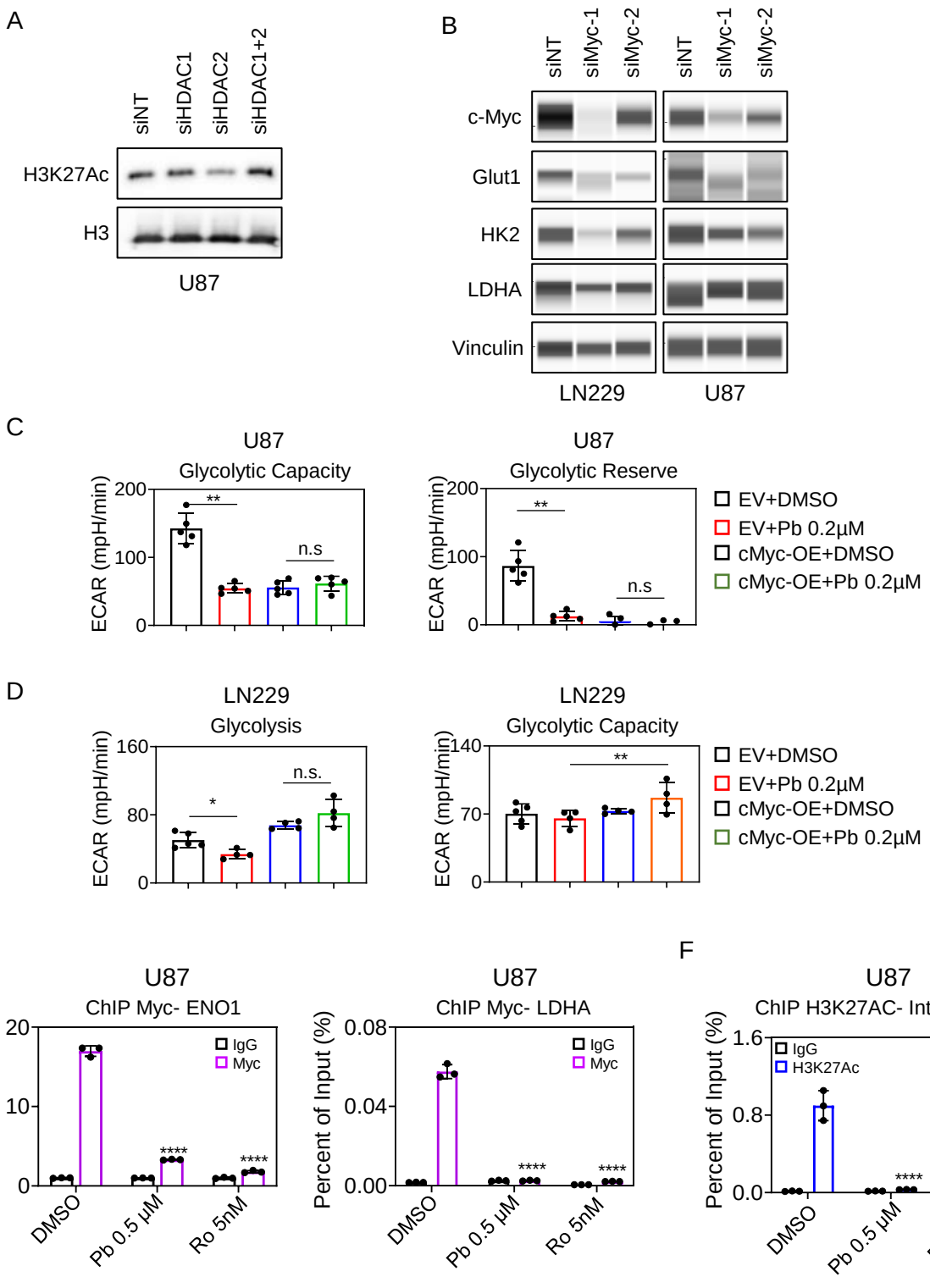
A
siNT
siHDAC1
siHDAC2
siHDAC1+2
H3K27Ac
H3
U87
B
siNT
siMyc-1
siMyc-2
siNT
siMyc-1
siMyc-2
c-Myc
Glut1
HK2
LDHA
Vinculin
LN229
U87
C
U87
Glycolytic Capacity
ECAR (mpH/min)
200
100
0
**
n.s
U87
Glycolytic Reserve
ECAR (mpH/min)
200
100
0
**
n.s
EV+DMSO
EV+Pb 0.2μM
cMyc-OE+DMSO
cMyc-OE+Pb 0.2μM
D
LN229
Glycolysis
ECAR (mpH/min)
160
80
0
*
n.s.
LN229
Glycolytic Capacity
ECAR (mpH/min)
140
70
0
**
EV+DMSO
EV+Pb 0.2μM
cMyc-OE+DMSO
cMyc-OE+Pb 0.2μM
E
U87
ChIP Myc- ENO1
Fold Change over IgG
20
10
0
IgG
Myc
****
****
DMSO
Pb 0.5 μM
Ro 5nM
U87
ChIP Myc- LDHA
Percent of Input (%)
0.08
0.04
0.00
IgG
Myc
****
****
DMSO
Pb 0.5 μM
Ro 5nM
F
U87
ChIP H3K27AC- Intron 1 Myc
Percent of Input (%)
1.6
0.8
0.0
IgG
H3K27Ac
****
****
DMSO
Pb 0.5 μM
Ro 5nM

Figure S5: HDAC inhibitors suppress c-Myc protein levels and thereby reduce glycolysis in GBM cells. (**A**) U87 GBM cells were transfected with siRNA against HDAC1, HDAC2 or the combination of both and analyzed for the indicated proteins by standard western blot. (**B**) Protein capillary electrophoresis from LN229 and U87 GBM cells that were transfected with two specific siRNAs against c-Myc. (**C**) Quantifications of glycolytic reserve or glycolytic capacity related ECAR production of U87 cells expressing c-Myc cDNA with 0.2 μM panobinostat treatments for 24h. Shown are means and SEM (n=5). (**D**) Quantifications of glycolysis or glycolytic capacity related ECAR production of LN229 cells expressing c-Myc with 0.2 μM panobinostat treatments for 24h. Shown are means and SEM (n=4-5). (**E**) Shown are CHIP-qPCRs (antibody c-Myc) of ENO1 or LDHA from U87 cells (n=3). (**F**) Shown are CHIP-qPCRs (antibody H3K27ac) of intron 1 MYC from U87 cells (n=3). Shown are means and SD. Statistical significance was determined by two-tailed Student's t-test (**C** and **D**) and by one-way ANOVA (**E** and **F**). *P < 0.05; **P < 0.01; ***/****P < 0.001.

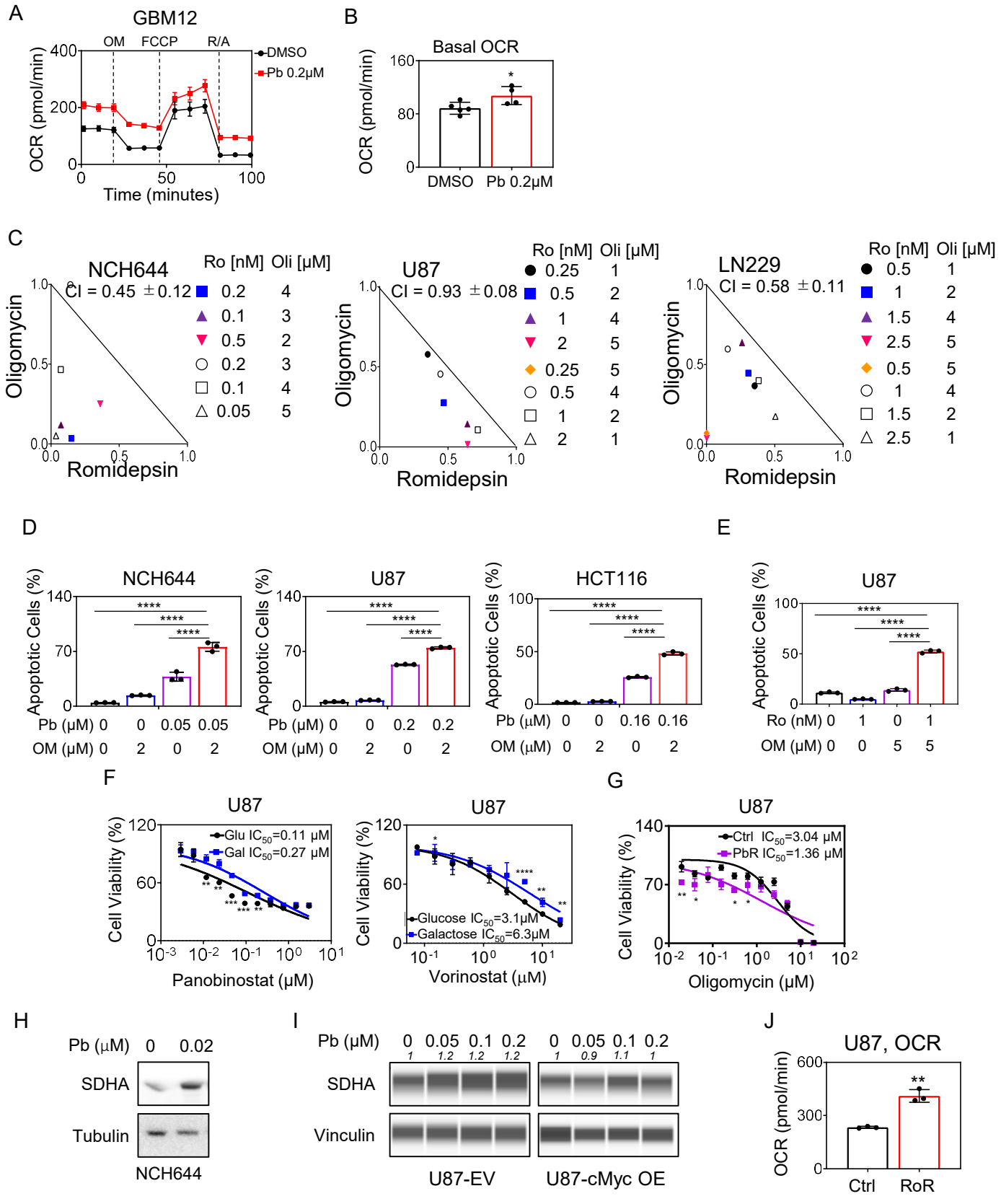
A
GBM12
OM
FCCP
R/A
DMSO
Pb 0.2μM
OCR (pmol/min)
Time (minutes)
B
Basal OCR
OCR (pmol/min)
DMSO
Pb 0.2μM
C
NCH644
CI = 0.45 ±0.12
Ro [nM] Oli [μM]
0.2 4
0.1 3
0.5 2
0.2 3
0.1 4
0.05 5
U87
CI = 0.93 ±0.08
Ro [nM] Oli [μM]
0.25 1
0.5 2
1 4
2 5
0.25 5
0.5 4
1 2
2 1
LN229
CI = 0.58 ±0.11
Ro [nM] Oli [μM]
0.5 1
1 2
1.5 4
2.5 5
0.5 5
1 4
1.5 2
2.5 1
Oligomycin
Romidepsin
D
NCH644
U87
HCT116
Apoptotic Cells (%)
Pb (μM) 0 0 0.05 0.05
OM (μM) 0 2 0 2
Pb (μM) 0 0 0.2 0.2
OM (μM) 0 2 0 2
Pb (μM) 0 0 0.16 0.16
OM (μM) 0 2 0 2
E
U87
Apoptotic Cells (%)
Ro (nM) 0 1 0 1
OM (μM) 0 0 5 5
F
U87
Cell Viability (%)
Glu IC50=0.11 μM
Gal IC50=0.27 μM
Panobinostat (μM)
U87
Glucose IC50=3.1μM
Galactose IC50=6.3μM
Vorinostat (μM)
G
U87
Ctrl IC50=3.04 μM
PbR IC50=1.36 μM
Oligomycin (μM)
H
Pb (μM) 0 0.02
SDHA
Tubulin
NCH644
I
Pb (μM) 0 0.05 0.1 0.2 0 0.05 0.1 0.2
1 1.2 1.2 1.2 1 0.9 1.1 1
SDHA
Vinculin
U87-EV
U87-cMyc OE
J
U87, OCR
OCR (pmol/min)
Ctrl
RoR

Figure S6: HDAC inhibitor exposure leads to activation of oxidative metabolism. (**A** and **B**) A mitostress extracellular flux analysis of GBM12 (PDX) GBM cells treated with 0.2 μM panobinostat for 24h. OM: oligomycin, R/A: rotenone and antimycin. Quantification of basal OCR is provided (B). Shown are means and SEM (n=4-5). (**C**) NCH644, U87 and LN229 GBM cells were treated with romidepsin in the presence of oligomycin for 72h and cellular viability was determined. Isobolograms are shown. (**D**) Quantifications of apoptotic cells from NCH644, U87 and HCT116 cells treated with panobinostat and oligomycin for 48h (n=3). (**E**) Quantifications of apoptotic cells from U87 GBM cells treated with 1 nM romidepsin and 5 μM oligomycin for 48h (n=3). (**F**) U87 cells were cultured in the presence of 25 mM glucose or 25 mM galactose for two weeks, then cells were treated with increasing concentrations of panobinostat or vorinostat for 72h and cellular viability was determined. IC_{50} values were calculated by non-linear regression method (n=4). (**G**) Parental or chronically exposed panobinostat U87 cells were treated with oligomycin for 72h and cellular viability was determined. IC_{50} values were calculated by non-linear regression method (n=3). (**H**) Standard western blot of NCH644 cells were treated with 20 nM panobinostat for 24h and analyzed for the indicated protein. (**I**) U87 cells transduced with c-Myc, exposed to panobinostat for 24h and analyzed for the indicated protein by capillary electrophoresis. (**J**) OCR analysis of parental or chronically exposed to romidepsin U87 cells (n=3). Shown are means and SD. Statistical significance was determined by two-tailed Student's t-test (**B** and **J**) and by one-way ANOVA (**D** and **E**). *P < 0.05; **P < 0.01; ***/****P < 0.001.

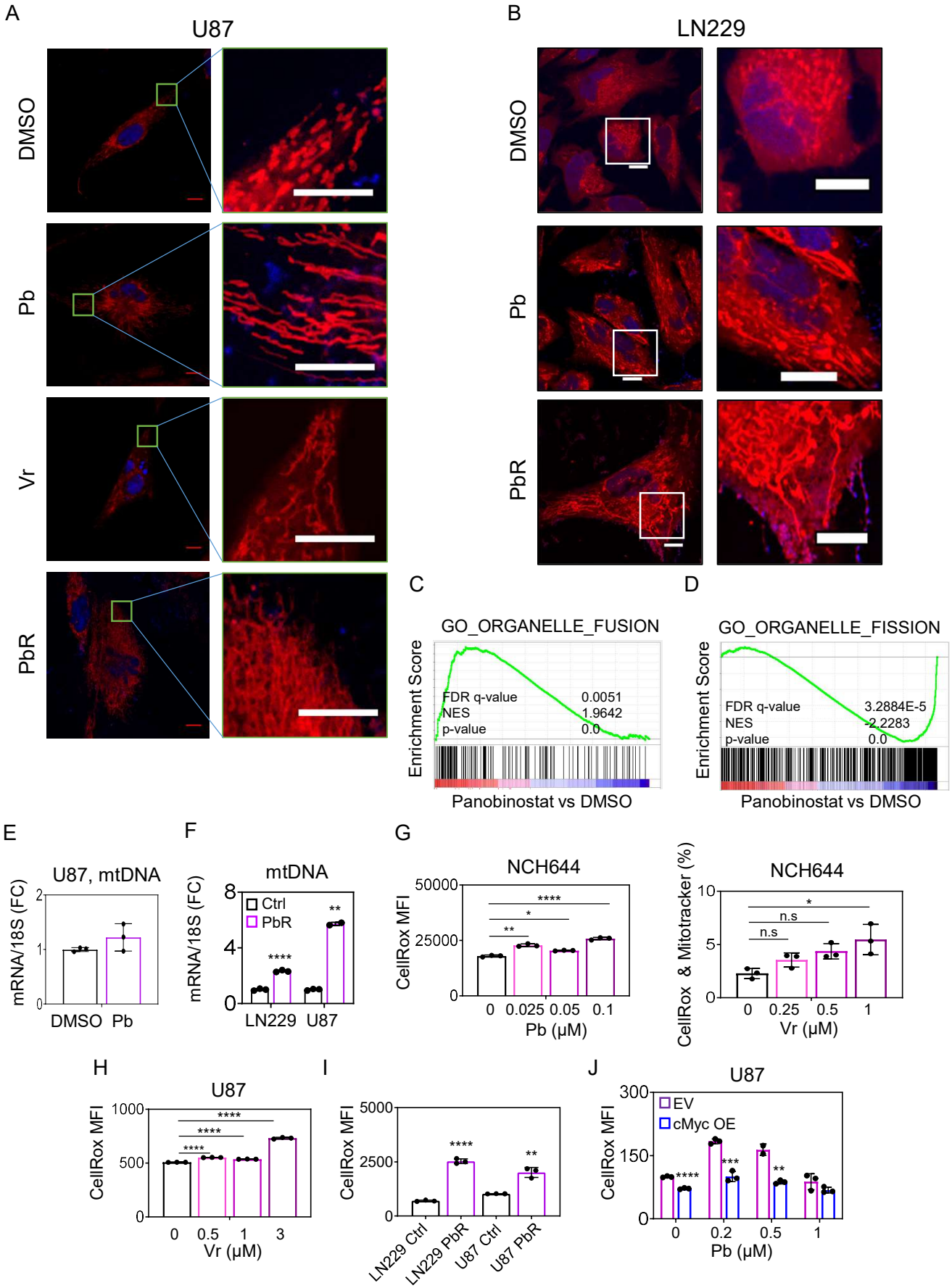
A
U87
DMSO
Pb
Vr
PbR
B
LN229
DMSO
Pb
PbR
C
GO_ORGANELLE_FUSION
Enrichment Score
FDR q-value 0.0051
NES 1.9642
p-value 0.0
Panobinostat vs DMSO
D
GO_ORGANELLE_FISSION
Enrichment Score
FDR q-value 3.2884E-5
NES -2.2283
p-value 0.0
Panobinostat vs DMSO
E
U87, mtDNA
mRNA/18S (FC)
DMSO Pb
F
mtDNA
mRNA/18S (FC)
Ctrl
PbR
LN229 U87
G
NCH644
CellRox MFI
Pb (μM)
NCH644
CellRox & Mitotracker (%)
n.s
Vr (μM)
H
U87
CellRox MFI
Vr (μM)
I
CellRox MFI
LN229 Ctrl
LN229 PbR
U87 Ctrl
U87 PbR
J
U87
CellRox MFI
EV
cMyc OE
Pb (μM)

Figure S7: HDAC inhibitor increases mitochondria number, mito-biogenesis and ROS production. (**A**) U87 cells were treated with panobinostat (Pb), vorinostat (Vr) or chronically exposed to panobinostat (PbR) U87 cells were labeled with mitotracker and subjected to confocal microscopy. Shown are representative cells of low (left) and high (right) magnification. Scale bar: 10 μm. (**B**) LN229 cells were treated with panobinostat (Pb) or chronically exposed to panobinostat (PbR) LN229 cells were labeled with mitotracker and subjected to confocal microscopy. Shown are representative cells of low (left) and high (right) magnification. Scale bar: 10μm. (**C** and **D**) NCH644 GBM cells were treated with panobinostat (Pb) and transcriptome and gene set enrichment analysis were performed. Shown are enrichment plots. NES: Normalized enrichment score. (**E**) mtDNA mRNA levels from U87 GBM cells were treated with panobinostat for 24h (n=3). (**F**) mtDNA mRNA levels from parental and chronically exposed panobinostat LN229 or U87 cells (n=2-3). (**G**) NCH644 GBM cells were treated with panobinostat or vorinostat, were stained with CellRox or CellRox and Mitotracker and analyzed by flow cytometry (n=3). (**H**) U87 GBM cells were treated with indicated concentrations of vorinostat, were stained with CellRox and analyzed by flow cytometry (n=3). (**I**) Parental or chronically panobinostat exposed U87 or LN229 cells were stained with CellRox and analyzed by flow cytometry (n=3). (**J**) U87 cells transduced with c-Myc were treated with panobinostat for 24h and analyzed by flow cytometry following CellRox staining (n=2-3). Shown are means and SD. Statistical significance was determined by two-tailed Student's t-test (**D** and **E**) and by one-way ANOVA (**F** and **J**). *P < 0.05; **P < 0.01; ***/****P < 0.001.

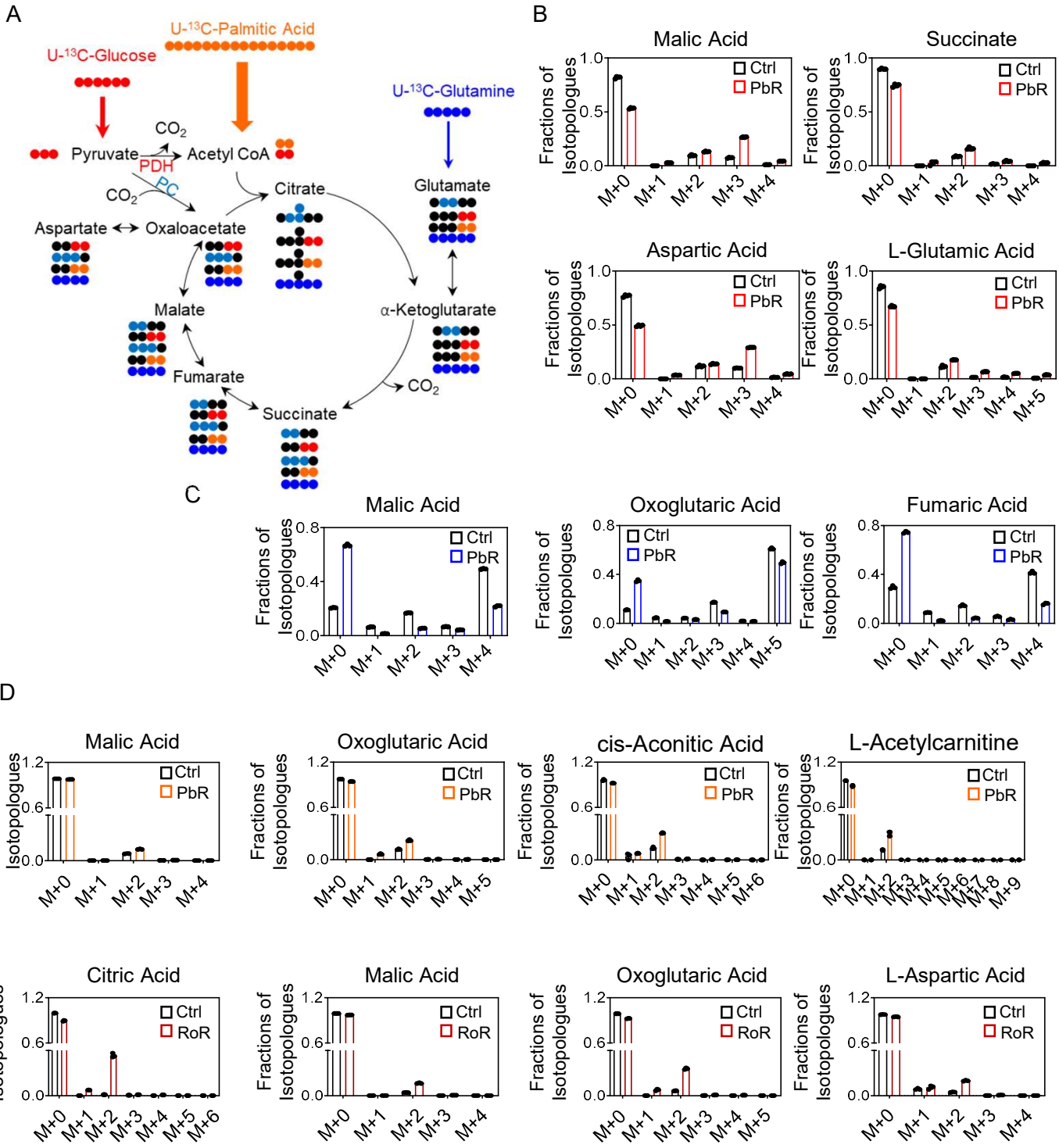
A
U-13C-Palmitic Acid
U-13C-Glucose
U-13C-Glutamine
CO2
Pyruvate
Acetyl CoA
PDH
PC
CO2
Citrate
Glutamate
Aspartate
Oxaloacetate
Malate
α-Ketoglutarate
Fumarate
CO2
Succinate
B
Malic Acid
Succinate
Aspartic Acid
L-Glutamic Acid
Fractions of Isotopologues
Ctrl
PbR
M+0
M+1
M+2
M+3
M+4
M+5
C
Malic Acid
Oxoglutaric Acid
Fumaric Acid
D
Malic Acid
Oxoglutaric Acid
cis-Aconitic Acid
L-Acetylcarnitine
M+6
M+7
M+8
M+9
E
Citric Acid
Malic Acid
Oxoglutaric Acid
L-Aspartic Acid
RoR

Figure S8: Pan-HDAC inhibitor alters carbon labeling (U-^{13}C-glucose, U-^{13}C-glutamine, U-^{13}C-palmitic acid) of TCA-cycle related metabolites. (A) An overview chart is shown to highlight the different routes of glucose, glutamine and palmitic acid carbons through the TCA cycle. PC: pyruvate carboxylase, PDH: pyruvate dehydrogenase (**B**) Parental or chronically exposed panobinostat U87 cells were cultured in DMEM media containing 25mM U-^{13}C-Glucose, 4mM Glutamine and 10% dialyzed FBS for 24h and subjected to LC/MS analysis (n=3). (**C**) Parental or chronically exposed panobinostat U87 cells were cultured in DMEM media containing 25mM Glucose, 4mM U-^{13}C-Glutamine and 10% dialyzed FBS for 24h and subjected to LC/MS analysis (n=3). (**D**) Parental or chronically exposed panobinostat U87 cells were cultured in DMEM media containing 5mM Glucose, 1mM Glutamine, 100 µM U-^{13}C-Palmitic acid and 10% dialyzed FBS for 24h and subjected to LC/MS analysis (n=3). (**E**) Parental or chronically exposed romidepsin U87 cells were cultured in DMEM media containing 5mM Glucose, 1mM Glutamine, 100 µM U-^{13}C-Palmitic acid and 10% dialyzed FBS for 24h and subjected to LC/MS analysis (n=3).

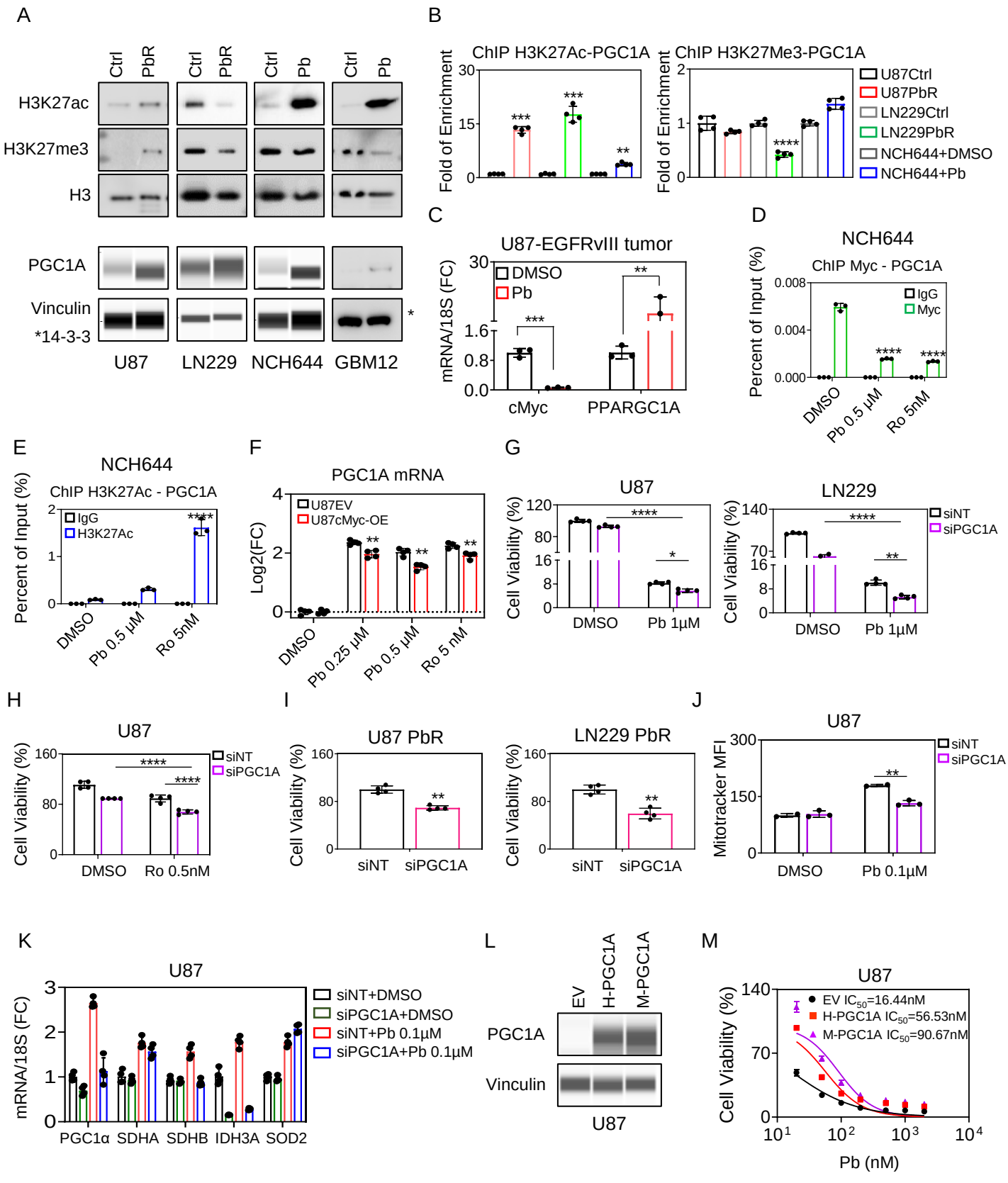
A
Ctrl
PbR
Ctrl
PbR
Ctrl
Pb
Ctrl
Pb
H3K27ac
H3K27me3
H3
PGC1A
Vinculin
*14-3-3
*
U87
LN229
NCH644
GBM12
B
ChIP H3K27Ac-PGC1A
Fold of Enrichment
30
15
0
***
***
**
ChIP H3K27Me3-PGC1A
Fold of Enrichment
2
1
0
****
U87Ctrl
U87PbR
LN229Ctrl
LN229PbR
NCH644+DMSO
NCH644+Pb
C
U87-EGFRvIII tumor
mRNA/18S (FC)
30
1.6
0.8
0.0
DMSO
Pb
***
**
cMyc
PPARGC1A
D
NCH644
ChIP Myc - PGC1A
Percent of Input (%)
0.008
0.004
0.000
IgG
Myc
****
****
DMSO
Pb 0.5 μM
Ro 5nM
E
NCH644
ChIP H3K27Ac - PGC1A
Percent of Input (%)
2
1
0
IgG
H3K27Ac
****
DMSO
Pb 0.5 μM
Ro 5nM
F
PGC1A mRNA
Log2(FC)
4
2
0
U87EV
U87cMyc-OE
**
**
**
**
DMSO
Pb 0.25 μM
Pb 0.5 μM
Ro 5 nM
G
U87
Cell Viability (%)
120
80
16
8
0
****
*
DMSO
Pb 1μM
LN229
Cell Viability (%)
140
70
16
8
0
****
**
siNT
siPGC1A
DMSO
Pb 1μM
H
U87
Cell Viability (%)
160
80
0
siNT
siPGC1A
****
****
DMSO
Ro 0.5nM
I
U87 PbR
Cell Viability (%)
160
80
0
**
siNT
siPGC1A
LN229 PbR
Cell Viability (%)
160
80
0
**
siNT
siPGC1A
J
U87
Mitotracker MFI
300
150
0
siNT
siPGC1A
**
DMSO
Pb 0.1μM
K
U87
mRNA/18S (FC)
3
2
1
0
siNT+DMSO
siPGC1A+DMSO
siNT+Pb 0.1μM
siPGC1A+Pb 0.1μM
PGC1α
SDHA
SDHB
IDH3A
SOD2
L
EV
H-PGC1A
M-PGC1A
PGC1A
Vinculin
U87
M
U87
Cell Viability (%)
140
70
0
EV IC50=16.44nM
H-PGC1A IC50=56.53nM
M-PGC1A IC50=90.67nM
10^1
10^2
10^3
10^4
Pb (nM)

Figure S9: PGC1A as a pro-survival factor in the context of HDAC inhibition. (**A**) Western blots from parental and chronically exposed panobinostat U87 or LN229 cells as well as NCH644 and GBM12 cells treated with panobinostat for 24h (H3K27ac, H3K27me3 and H3 (loading control): standard WB; PGC1A and Vinculin (loading control): protein capillary electrophoresis; PGC1A and 14-3-3 (loading control): standard WB in GBM12). * indicates 14-3-3. (**B**) CHIP-qPCR analysis of the PGC1A promoter with either H3K27ac antibody (left) or H3K27me3 antibody (right). (**C**) U87-EGFRvIII xenografted tumors were treated with panobinostat and RT-PCR analysis was performed for c-Myc and PGC1A (n=3). (**D** and **E**) CHIP-qPCR analysis of the PGC1A promoter from NCH644 cells with c-Myc antibody or H3K27ac antibody (n=3). (**F**) PGC1A mRNA levels from U87 cells transduced with a c-Myc construct and treated with panobinostat/romidepsin for 24h (n=4). (**G**) U87 and LN229 cells were transfected with siRNA PGC1A, treated with 1µM panobinostat and cellular viability was determined (n=4). (**H**) U87 cells were transfected with PGC1A siRNA, treated with 0.5 nM romidepsin and cellular viability was determined (n=4). (**I**) Chronically exposed panobinostat U87 or LN229 cells were transfected with PGC1A siRNA and cellular viability was determined (n=4). (**J**) U87 cells were transfected with PGC1A siRNA, treated with panobinostat for 24h and analyzed Mitotracker (n=4). (**K**) U87 cells were transfected with PGC1A siRNA and treated with 0.1 µM panobinostat (n=4). RNA was isolated and real-time PCR analysis was performed for the indicated genes. (**L**) Protein capillary electrophoresis of U87 cells expressing human or mouse PGC1A. (**M**) U87 cells expressing human or mouse PGC1A, treated with panobinostat and cellular viability was determined. IC_{50} values were calculated by non-linear regression method (n=4). Shown are means and SD. Statistical significance was determined by two-tailed Student's t-test (**B, C, F** and **I**) and by one-way ANOVA (**D, E, G, H,** and **J**). *P < 0.05; **P < 0.01; ***/****P < 0.001.

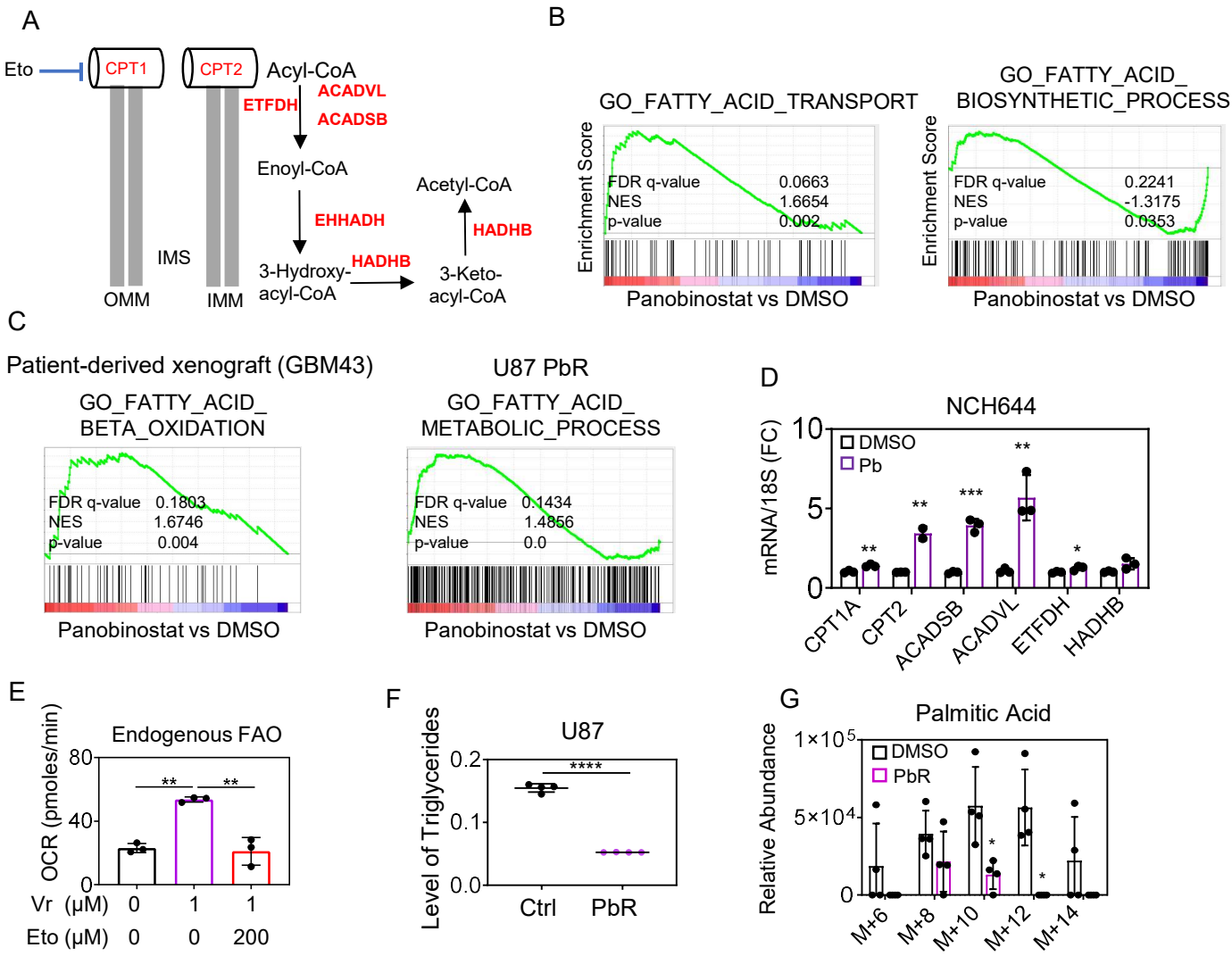
A
Eto
CPT1
CPT2
Acyl-CoA
ACADVL
ETFDH
ACADSB
Enoyl-CoA
EHHADH
Acetyl-CoA
HADHB
IMS
HADHB
3-Hydroxy-acyl-CoA
3-Keto-acyl-CoA
OMM
IMM
B
GO_FATTY_ACID_TRANSPORT
Enrichment Score
FDR q-value 0.0663
NES 1.6654
p-value 0.002
Panobinostat vs DMSO
GO_FATTY_ACID_ BIOSYNTHETIC_PROCESS
Enrichment Score
FDR q-value 0.2241
NES -1.3175
p-value 0.0353
Panobinostat vs DMSO
C
Patient-derived xenograft (GBM43)
GO_FATTY_ACID_ BETA_OXIDATION
FDR q-value 0.1803
NES 1.6746
p-value 0.004
Panobinostat vs DMSO
U87 PbR
GO_FATTY_ACID_ METABOLIC_PROCESS
FDR q-value 0.1434
NES 1.4856
p-value 0.0
Panobinostat vs DMSO
D
NCH644
mRNA/18S (FC)
DMSO
Pb
CPT1A
CPT2
ACADSB
ACADVL
ETFDH
HADHB
E
Endogenous FAO
OCR (pmoles/min)
Vr (μM) 0 1 1
Eto (μM) 0 0 200
F
U87
Level of Triglycerides
Ctrl
PbR
G
Palmitic Acid
Relative Abundance
DMSO
PbR
M+6
M+8
M+10
M+12
M+14

Figure S10: HDAC inhibition results in reprogramming of lipid metabolism. (A) The diagram highlights the necessary components of beta-oxidation, including transporters, CPT1A and CPT2, with an associated inhibitor etomoxir as well as enzymes. OMM: outer mitochondrial membrane, IMS: inter membrane space, IMM: inner mitochondrial membrane. Transporters or enzymes highlighted in red are increased post panobinostat treatment based on gene set enrichment analysis or real-time PCR analysis. (**B**) NCH644 cells were treated with 0.5 μM panobinostat for 24h. RNA was isolated and subjected to transcriptome and gene set enrichment analysis. Shown are gene set enrichment plots related to lipid metabolism. NES: Normalized enrichment score. (**C**) GBM43 PDX tumors were treated as described in figure 7 (left) and subjected to transcriptome analysis. Parental and chronically panobinostat exposed U87 GBM cells were subjected to transcriptome analysis (right). (**D**) NCH644 cells were treated with 0.5 μM panobinostat for 24h. RNA was isolated and real-time PCR analysis was performed for the indicated genes (n=2-3). (**E**) Quantifications of OCR in the context of a fatty acid oxidation assay measured by extracellular flux analysis with U87 GBM cells treated with the indicated drugs for 24h (n=3). (**F)** Triglyceride levels of parental and chronically panobinostat exposed U87 cells by LC/MS analysis of the lipid fraction. (**G**) Quantifications of relative abundance of ^{13}C labeled palmitic acid of parental and chronically exposed U87 cells incubated with 25 mM U-^{13}C-glucose (n=4). Shown are means and SD. Statistical significance was determined by two-tailed Student's t-test (**D, F,** and **G**) and by one-way ANOVA (**E**). *P < 0.05; **P < 0.01; ***/****P < 0.001.

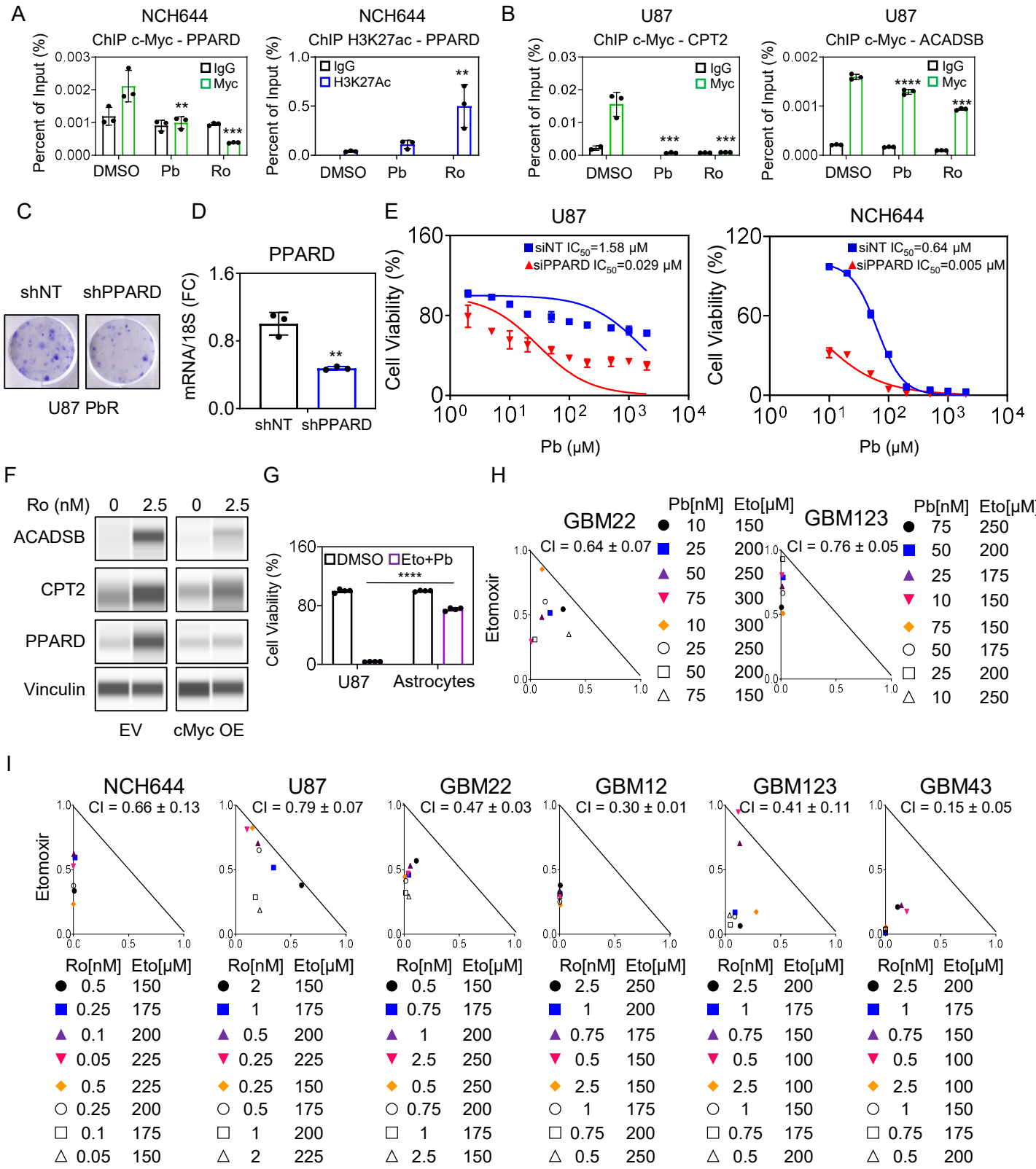
A
NCH644
ChIP c-Myc - PPARD
Percent of Input (%)
IgG
Myc
DMSO
Pb
Ro
NCH644
ChIP H3K27ac - PPARD
IgG
H3K27Ac
B
U87
ChIP c-Myc - CPT2
U87
ChIP c-Myc - ACADSB
C
shNT
shPPARD
U87 PbR
D
PPARD
mRNA/18S (FC)
E
U87
siNT IC50=1.58 μM
siPPARD IC50=0.029 μM
Cell Viability (%)
Pb (μM)
NCH644
siNT IC50=0.64 μM
siPPARD IC50=0.005 μM
F
Ro (nM) 0 2.5 0 2.5
ACADSB
CPT2
PPARD
Vinculin
EV
cMyc OE
G
DMSO
Eto+Pb
U87
Astrocytes
H
GBM22
CI = 0.64 ± 0.07
GBM123
CI = 0.76 ± 0.05
Etomoxir
Pb[nM] Eto[μM]
10 150
25 200
50 250
75 300
10 300
25 250
50 200
75 150
75 250
50 200
25 175
10 150
75 150
50 175
25 200
10 250
I
NCH644
CI = 0.66 ± 0.13
U87
CI = 0.79 ± 0.07
GBM22
CI = 0.47 ± 0.03
GBM12
CI = 0.30 ± 0.01
GBM123
CI = 0.41 ± 0.11
GBM43
CI = 0.15 ± 0.05
Ro[nM] Eto[μM]
0.5 150
0.25 175
0.1 200
0.05 225
0.5 225
0.25 200
0.1 175
0.05 150
2 150
1 175
0.5 200
0.25 225
0.25 150
0.5 175
1 200
2 225
0.5 150
0.75 175
1 200
2.5 250
0.5 250
0.75 200
1 175
2.5 150
2.5 250
1 200
0.75 175
0.5 150
2.5 150
1 175
0.75 150
0.5 100
2.5 100
1 150
0.75 175
0.5 200
2.5 200
1 175
0.75 150
0.5 100
2.5 100
1 150
0.75 175
0.5 200

Figure S11: The combination treatment of HDAC inhibitors along with etomoxir reduces the cellular viability of PDX GBM cells in a synergistic manner. **(A)** CHIP-qPCR analysis of the PPARD promoter from NCH644 GBM cell lysates with either c-Myc antibody (left) or H3K27ac antibody (right) (n=3). (**B**) CHIP-qPCR analysis of the CPT2 or ACADSB promoter (c-Myc binding region) from U87 cell lysate with c-Myc antibody chromatin immunoprecipitation (n=3). (**C**) Representative photos of colony forming assay from U87 PbR cells with specific PPARD shRNA lentivirus transduction. (**D**) PPARD mRNA levels from U87 PbR cells specific PPARD shRNA lentivirus transduction (n=3). (**E**) U87 and NCH644 GBM cells were transfected with siPPARD and treated with indicated concentrations of panobinostat for 72h and cellular viability was determined. IC_{50} values were calculated by non-linear regression method (n=4). (**F**) U87 cells were transduced with a c-Myc construct, were treated with 2.5 nM romidepsin for 24h and analyzed for the indicated proteins. (**G**) U87 GBM cells and astrocytes were treated with etomoxir and panobinostat for 72h and cellular viability was determined (n=4). (**H**) GBM22 and GBM123 were treated with etomoxir and panobinostat for 72h and cellular viability was determined. Shown are the isobolograms (n=4). (**I**) U87, NCH644 stem-like GBM cells and PDX-lines (GBM22, GBM12, GBM123 and GBM43) were treated with etomoxir and romidepsin for 72h and cellular viability was determined. Shown are the isobolograms (n=4). Shown are means and SD. Statistical significance was determined by two-tailed Student's t-test (**D** and **G**) and by one-way ANOVA (**A** and **B**). **P < 0.01; ***/****P < 0.001.

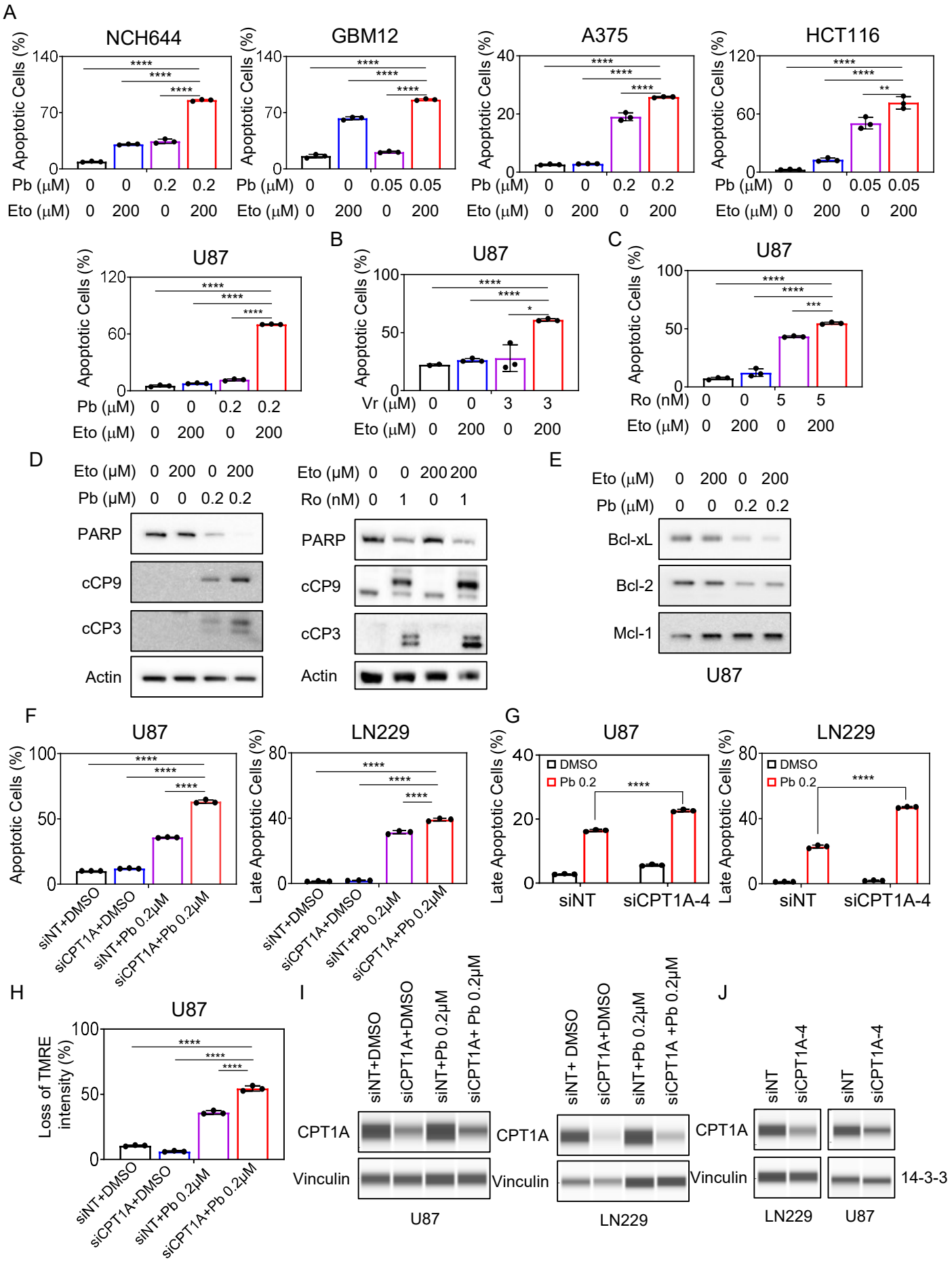
A
NCH644
GBM12
A375
HCT116
Apoptotic Cells (%)
Pb (μM)
Eto (μM)
U87
B
Vr (μM)
C
Ro (nM)
D
PARP
cCP9
cCP3
Actin
Ro (nM)
E
Bcl-xL
Bcl-2
Mcl-1
F
LN229
Late Apoptotic Cells (%)
siNT+DMSO
siCPT1A+DMSO
siNT+Pb 0.2μM
siCPT1A+Pb 0.2μM
G
DMSO
Pb 0.2
siNT
siCPT1A-4
H
Loss of TMRE intensity (%)
I
CPT1A
Vinculin
siNT+ DMSO
siCPT1A +Pb 0.2μM
J
14-3-3

Figure S12: CPT1A silencing enhances the apoptotic effects of HDAC inhibitors. (**A**) Stem-like NCH644, GBM12 (PDX), A375 melanoma, HCT116 colonic carcinoma, and U87 GBM cells were treated with etomoxir (Eto) and panobinostat (Pb) for 48h, stained with PI/Annexin V and analyzed by flow cytometry (n=3). (**B**) U87 GBM cells were treated with etomoxir and vorinostat for 48h, stained with PI/Annexin V and analyzed by flow cytometry (n=3). (**C**) U87 cells were treated with etomoxir and romidepsin for 48h, stained with PI/Annexin V and analyzed by flow cytometry (n=3). (**D**) Standard western blots of proteins from U87 GBM cells treated with etomoxir, panobinostat/romidepsin or the combination of both for 24h. (**E**) Standard western blots of proteins from U87 cells treated with etomoxir, panobinostat or the combination of both for 24h. (**F**) U87 and LN229 cells were transfected with CPT1A siRNA, treated with 0.2 µM panobinostat for 48h, stained with PI/Annexin V and analyzed by flow cytometry (n=3). (**G**) U87 and LN229 cells were transfected with CPT1A-4 siRNA, treated with 0.2 µM panobinostat for 48h, stained with PI/Annexin V and analyzed by flow cytometry (n=3). (**H**) U87 GBM cells were transfected with CPT1A siRNA, treated with 0.2 µM panobinostat for 48h, stained with TMRE and analyzed by flow cytometry (n=3). (**I)** Protein capillary electrophoresis of proteins from U87 and LN229 cells transfected CPT1A siRNA and treated with 0.2 µM panobinostat for 48h. (**J**) Protein capillary electrophoresis from U87 and LN229 cells transfected with CPT1A-4 siRNA. Shown are means and SD. Statistical significance was determined by two-tailed Student's t-test (**G**) and by one-way ANOVA (**A-C, F** and **H**). *P<0.05; **P < 0.01; ***/****P < 0.001.

A

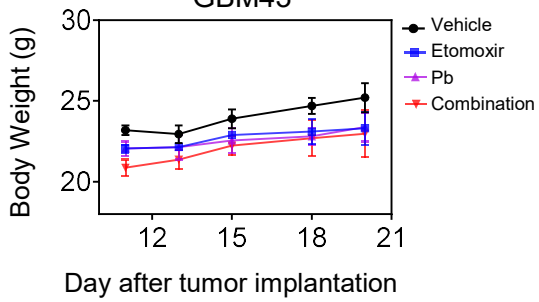
GBM43
Body Weight (g)
30
25
20
12
15
18
21
Vehicle
Etomoxir
Pb
Combination
Day after tumor implantation

C

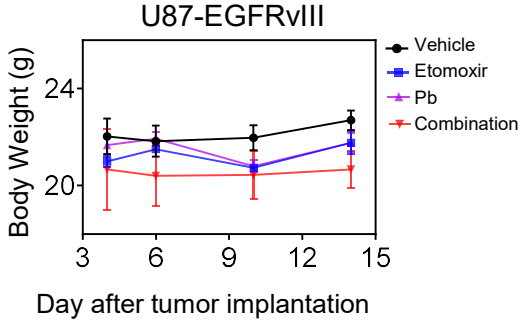
U87-EGFRvIII
Body Weight (g)
24
20
3
6
9
12
15
Vehicle
Etomoxir
Pb
Combination
Day after tumor implantation

B

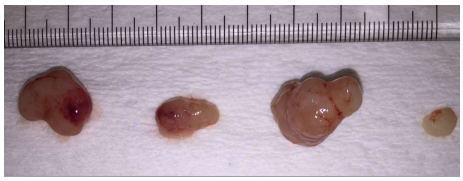
GBM43
Vehicle
Etomoxir
Pb
Combination

D

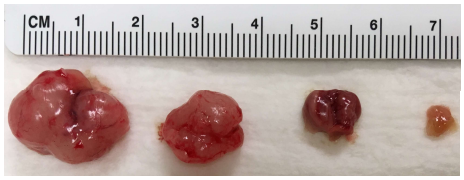
U87 EGFRvIII
CM
1
2
3
4
5
6
7
Vehicle
Etomoxir
Pb
Combination

E

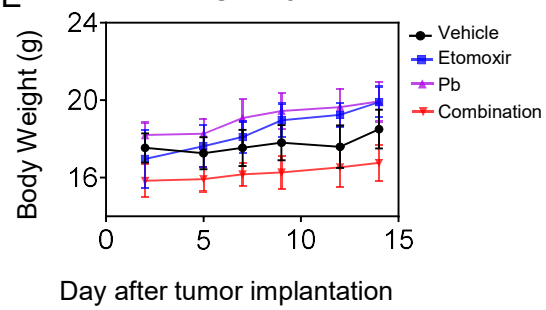
HCT116
Body Weight (g)
24
20
16
0
5
10
15
Vehicle
Etomoxir
Pb
Combination
Day after tumor implantation

G

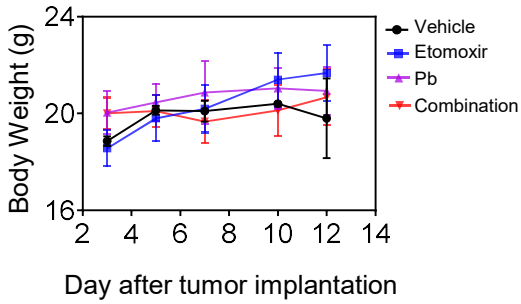
A375
Body Weight (g)
24
20
16
2
4
6
8
10
12
14
Vehicle
Etomoxir
Pb
Combination
Day after tumor implantation

F

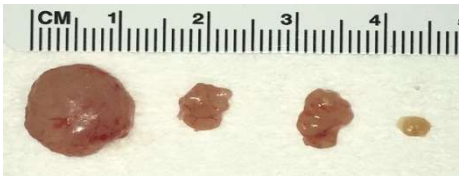
CM
1
2
3
4
Vehicle
Etomoxir
Pb
Combination

H

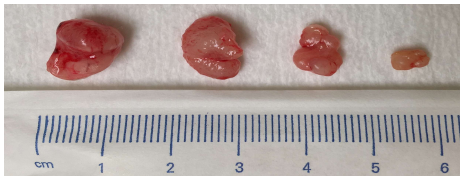
cm
1
2
3
4
5
6
Vehicle
Etomoxir
Pb
Combination

Figure S13: The combination treatment of etomoxir and panobinostat shows no detectable toxicity by body weight measurements. (**A**) Body weight curves from the indicated experiments in Figure 7A (n=2-3). (**B**) Photos of representative tumors at the final time point of each models in Figure 7A. (**C**) Body weight curves from the indicated experiments in Figure 7C (n=3). (**D**) Photos of representative tumors at the final time point of each models in Figure 7C. (**E**) Body weight curves from the indicated experiments in Figure 7E (n=3). (**F**) Photos of representative tumors at the final time point of each models in Figure 7E. (**G**) Body weight curves from the indicated experiments in Figure 7G (n=3). (**H**) Photos of representative tumors at the final time point of each models in Figure 7G. Shown are means and SD.

Supplementary Table 1

Primer sequences for real time PCR and chromatin immunoprecipitation qPCR

qPCR primer hGLUT1_Fw:	TTGCAGGCTTCTCCAACTGGAC
qPCR primer hGLUT1 Rv:	CAGAACCAGGAGCACAGTGAAG
qPCR primer hHK2 Fw:	CGGCCGTGCTACAATAGG
qPCR primer hHK2 Rv:	CTCGGGATCATGTGAGGG
qPCR primer hPFKL Fw:	AAGAAGTAGGCTGGCACGACGT
qPCR primer: hPFKL Rv:	GCGGATGTTCTCCACAATGGAC
qPCR primer: hGAPDH Fw:	GTCTCCTCTGACTTCAACAGCG
qPCR primer: hGAPDH Rv:	ACCACCCTGTTGCTGTAGCCAA
qPCR primer: hENO1 Fw:	AGTCAACCAGATTGGCTCCGTG
qPCR primer: hENO1 Rv:	CACAACCAGGTCAGCGATGAAG
qPCR primer: hLDHA Fw:	GGATCTCCAACATGGCAGCCTT
qPCR primer: hLDHA Rv:	AGACGGCTTTCTCCCTCTTGCT
qPCR primer: hMyc Fw:	CCTGGTGCTCCATGAGGAGAC
qPCR primer: hMyc Rv:	CAGACTCTGACCTTTTGCCAGG
qPCR primer: hPPARGC1A Fw:	CCAAAGGATGCGCTCTCGTTCA
qPCR primer: hPPARGC1A Rv:	CGGTGTCTGTAGTGGCTTGACT
qPCR primer: hmtDNA Fw:	CGAAAGGACAAGAGAAATAAGG
qPCR primer: hmtDNA Rv:	CTGTAAAGTTTTAAGTTTTATGCG
qPCR primer: hCPT1A Fw:	GATCCTGGACAATACCTCGGAG
qPCR primer: hCPT1A Rv:	CTCCACAGCATCAAGAGACTGC
qPCR primer: hCPT2 Fw:	GCAGATGATGGTTGAGTGCTCC
qPCR primer: hCPT2 Rv:	AGATGCCGCAGAGCAAACAAGTG
qPCR primer: hACADSB Fw:	GCCACCTATTTGCCTCAGCTCA
qPCR primer: hACADSB Rv:	GCTCAGCACTGCTGATCCACAT
qPCR primer: hACADVL Fw:	TAGGAGAGGCAGGCAAACAGCT
qPCR primer: hACADVL Rv:	CACAGTGGCAAACTGCTCCAGA
qPCR primer: hETFDH Fw:	GGAAACACCATCCTAGCATTCGG
qPCR primer: hETFDH Rv:	CCACCAGGAAAGGTGAGTTTTGG
qPCR primer: hHADHB Fw:	CACAGTCTAGCCAAGAAGGCAC
qPCR primer: hHADHB Rv:	CATCTGCTCCAGTGAGGAAGGA
qPCR primer: hPPARD Fw:	GGCTTCCACTACGGTGTTCATG
qPCR primer: hPPARD Rv:	CTGGCACTTGTTGCGGTTCTTC
qPCR primer: hSOD2 Fw:	TAGGGCTGAGGTTTGTCCAG
qPCR primer: hSOD2 Rv:	GGAGAAGTACCAGGAGGCGT
qPCR primer: hTXNIP Fw:	CAGCAGTGCAAACAGACTTCGG
qPCR primer: hTXNIP Rv:	CTGAGGAAGCTCAAAGCCGAAC
qPCR primer: hDRP1 Fw:	GATGCCATAGTTGAAGTGGTGAC
qPCR primer: hDRP1 Rv:	CCACAAGCATCAGCAAAGTCTGG
qPCR primer: hFIS1 Fw:	CAAGGAACTGGAGCGGCTCATT
qPCR primer: hFIS1 Rv:	GGACACAGCAAGTCCGATGAGT
ChIP qPCR primer: PGC1A Fw:	CTGTGGCATTCAAAGCTGG
ChIP qPCR primer: PGC1A Rv:	CTTGCTGCTCTAACTCGTGAC

ChIP qPCR primer: HK2 exon 1 Fw:	GATTGCCTCGCATCTGC
ChIP qPCR primer: HK2 exon 1 Rv:	TTTGCCAGAGCCCAGC
ChIP qPCR primer: HK2 promoter region Fw:	CACATTGTTGCATGAAACTCC
ChIP qPCR primer: HK2 promoter region Rv:	GACCTCTCCGATTCACAGG
ChIP qPCR primer: PGC1A promoter Fw:	CTGGGTGTGCGTCTGTTTG
ChIP qPCR primer: PGC1A promoter Rv:	CGGCGTGGTCTGATTTAGTG
ChIP qPCR primer: PPARD_F2 Fw:	GCTACGTCCGCATCCCGCACC
ChIP qPCR primer: PPARD_R2 Rv:	CGAGACGTCACCGCGCTGCTC
ChIP qPCR primer: ENO1 Fw:	CGCACGTGCTGGGCCCCCG
ChIP qPCR primer: ENO1 Rv:	GGCCTGAGTGGCCACCGCCG
ChIP qPCR primer: LDHA Fw:	CTGACTCAGGCTCATGGCTCC
ChIP qPCR primer: LDHA Rv:	CGGCGGACGTGCGGGAACC

Supplementary Materials and Methods

CHIP-sequencing data analysis

Sequencing data was mapped to the human genome (hg38), using bowtie. Mapped sequenced data was subjected to peak calling, utilizing MACS2. The experiment is deposited (GSE124877 and GSE144399). Super-enhancers were quantified and called through utilization of a slightly modified strategy initially proposed by Whyte et al. 2013. Primer sequences are in the Table 1 (Supplementary Figure S1).

For peak calling, raw sequencing reads were aligned to the human genome HG38 using BWA MEM. PCR duplicates were removed using Picard MarkDuplicates (Picard Tools 1.90). Peaks were called against inputs using Macs2 (1). Normalized bedgraph tracks were generated using the SPMR flag and converted to bigWig using UCSC tool bedGraphToBigWig (2). Peaks with a score >5 were retained.

For peak differential statistics, bedtools merge was performed to quantitatively measure changes in epigenetic enrichment (3). Enrichment levels for each merged peak were quantified with featureCounts (4) as raw counts and normalized to counts per million (CPM) for comparison between samples. Differential expression statistics (fold-change and p-value) were computed using edgeR (5). P-values were adjusted for multiple testing using the false discovery rate (FDR) correction of Benjamini and Hochberg.

To identify super enhancers, Bedtools merge was performed to combine overlapping peaks within 12.5Kb distance, peak re-enrichment, normalization and subtracted input (control) peak signals. Merged peaks (super-enhancers) were then annotated, sorted and plotted for peak signals versus rank ordering. The normalized enrichment scores were obtained for 5 kb upstream or downstream of the peaks of super-enhancers, and heatmaps were generated using the normalized enrichment scores.

References:

1. Zhang Y, Liu T, Meyer CA, Eeckhoute J, Johnson DS, Bernstein BE, et al. Model-based analysis of ChIP-Seq (MACS). Genome Biol. 2008;9(9):R137.

2. Kent WJ, Zweig AS, Barber G, Hinrichs AS, and Karolchik D. BigWig and BigBed: enabling browsing of large distributed datasets. Bioinformatics. 2010;26(17):2204-7.

3. Quinlan AR, and Hall IM. BEDTools: a flexible suite of utilities for comparing genomic features. Bioinformatics. 2010;26(6):841-2.

4. Liao Y, Smyth GK, and Shi W. featureCounts: an efficient general purpose program for assigning sequence reads to genomic features. Bioinformatics. 2014;30(7):923-30.

5. McCarthy DJ, Chen Y, and Smyth GK. Differential expression analysis of multifactor RNA-Seq experiments with respect to biological variation. Nucleic Acids Res. 2012;40(10):4288-97.